

Structure and Magnetic Properties of Fe–B–Si–Zr Metallic Glasses

R. BABILAS^{a,*}, A. RADOŃ^a AND P. GEĘBARA^b

^aInstitute of Engineering Materials and Biomaterials, Silesian University of Technology,
S. Konarskiego 18a, 44-100 Gliwice, Poland

^bInstitute of Physics, Czestochowa University of Technology, al. Armii Krajowej 19, 42-200 Czestochowa, Poland

Fe-based amorphous alloys were characterized by X-ray diffraction, transmission Mössbauer spectroscopy and vibrating sample magnetometry. The studies were performed on $(\text{Fe}_{0.75}\text{B}_{0.15}\text{Si}_{0.1})_{100-x}\text{Zr}_x$ ($x = 0, 1, 3$) metallic glasses in the form of ribbons. The glassy samples were prepared by the “melt spinning” technique in argon protective atmosphere. The XRD patterns show the broad diffraction halo that is typical for amorphous Fe-based alloys. The Mössbauer spectroscopy allows to study the local environments of the Fe atoms in the glassy state, showing the changes in the amorphous structure due to the changing of Zr addition. From hysteresis loops obtained from vibrating sample magnetometry measurements, coercive force and saturation magnetization were determined versus different Zr content. The obtained magnetic properties allow to classify the studied amorphous alloys in as-cast state as soft magnetic materials.

DOI: [10.12693/APhysPolA.131.726](https://doi.org/10.12693/APhysPolA.131.726)

PACS/topics: 33.45.+x, 61.05.cp, 64.70.pe, 75.50.Kj

1. Introduction

Fe-based alloys are usually classified as a promising group of engineering materials due to their physicochemical properties and relatively low cost of production [1, 2]. These alloys show attractive soft magnetic behavior and can be used as precursors for the preparation of nanocrystalline alloys [3]. Recently, good glass-forming ability and high magnetic saturation was observed in Fe–Zr–B and Fe–Nb–B alloys. Therefore, Inoue and Shen revealed that the Fe-based amorphous alloys with Zr addition exhibited a saturation magnetization with a value of above 1.5 T [4]. They reported that Zr as paramagnetic element decreased the saturation magnetization, but also increased a crystallization temperature. Similar results were obtained by Geng et al. [5] who stated that the addition of Zr to Fe–Si–B glass allowed to obtain samples with diameter of 2.5 mm and coercivity of about 3 A/m. Because magnetic properties of metallic glasses are formed by their structure many experimental and computational methods including X-ray diffraction, the Mössbauer spectroscopy, nuclear magnetic resonance, reverse Monte Carlo modeling and molecular dynamics were used [6]. Nevertheless, a reconstruction of the atomic structure for metallic glasses is still difficult.

The aim of the paper is an attempt to describe a correlation between the local structure and selected magnetic properties of Fe–Si–B–Zr glasses.

2. Experimental

The studies were conducted on $\text{Fe}_{75}\text{B}_{15}\text{Si}_{10}$, $\text{Fe}_{74.25}\text{B}_{14.85}\text{Si}_{9.9}\text{Zr}_1$ and $\text{Fe}_{72.75}\text{B}_{14.55}\text{Si}_{9.7}\text{Zr}_3$ me-

tallic glasses in the form of ribbons with the thickness of 0.05 mm and the width of 3–6 mm. The ingots of studied master alloys were prepared by induction melting of the mixtures of pure elements. The amorphous ribbons were prepared by the melt spinning at a copper wheel surface speed of 30 m/s.

The structure of the ribbons in as-cast state was examined by X-ray diffraction in reflection mode using Seifert-FPM XRD7 diffractometer with $\text{Co } K_\alpha$ radiation. The diffraction patterns were collected by “step-scanning” method in the 2θ range from 30° to 90° . The room temperature hysteresis loops were measured by LakeShore 7307 vibrating sample magnetometer in magnetic fields up to 2 T. The coercive force was measured with error less than 1 A/m. The Mössbauer spectra were measured at room temperature using Polon Mössbauer spectrometer with a $^{57}\text{Co}:\text{Rh}$ source of the activity of 50 mCi in transmission geometry. The analysis was carried out using thin absorber approximation. The Mössbauer spectra were fitted with the WinNORMOS [7] for Igor 6.04 package.

3. Results and discussion

The X-ray diffraction patterns of the ribbons in the as-cast state are presented in Fig. 1. Each of the diffraction patterns manifest only a broad peak in the vicinity of $2\theta = 52^\circ$, which implies the formation of a single Fe-based glassy phase. No reflections of crystalline precipitations were detected. The X-ray measurements were carried out on a side of the ribbon that has not contact with the copper based wheel. Figure 2 shows magnetic hysteresis loops of the $(\text{Fe}_{0.75}\text{B}_{0.15}\text{Si}_{0.1})_{100-x}\text{Zr}_x$ glassy ribbons. Additionally, the inset in Fig. 2 presents a zoom of the loops, which allows to determine of coercive force values. Values of the saturation magnetization (J_s) were found to be 1.58, 1.44, and 1.49 T for the $x = 0, 1,$

*corresponding author; e-mail: rafal.babilas@polsl.pl

and 3, respectively, under an applied magnetic field of 800 kA/m. The addition of Zr caused a decrease of the coercive force (H_c) from 247 A/m for $\text{Fe}_{75}\text{B}_{15}\text{Si}_{10}$ glass to 168 A/m for alloy with 1 at.% of Zr addition. The lowest coercive force ($H_c = 64$ A/m) was obtained for the alloy $x = 3$. This decreasing tendency is similar to those revealed by Geng et al. [5] in Fe–Si–B–Zr metallic glasses. Moreover, Table I summarizes the examined magnetic properties for the melt-spun ribbons.

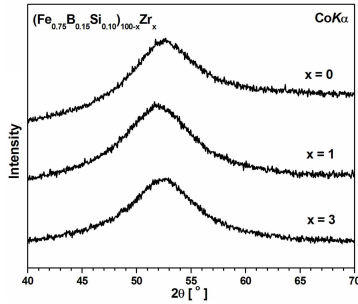


Fig. 1. X-ray diffraction patterns of $(\text{Fe}_{0.75}\text{B}_{0.15}\text{Si}_{0.1})_{100-x}\text{Zr}_x$ ($x = 0, 1, 3$) alloys in the form of ribbons in as-cast state.

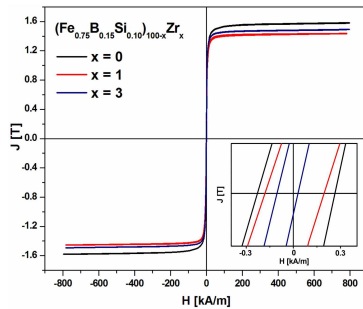


Fig. 2. Magnetic hysteresis loops of $(\text{Fe}_{0.75}\text{B}_{0.15}\text{Si}_{0.1})_{100-x}\text{Zr}_x$ ($x = 0, 1, 3$) alloys in the form of ribbons in as-cast state with inset of enlarged loops in the low magnetic field and magnetization ranges.

TABLE I

Magnetic properties of $(\text{Fe}_{0.75}\text{B}_{0.15}\text{Si}_{0.1})_{100-x}\text{Zr}_x$ alloys. J_s — saturation magnetization, H_c — coercive force.

x [at.%]	J_s [T]	H_c [A/m]
0	1.58	247
1	1.44	168
3	1.49	64

The magnetic behavior of studied alloys was further investigated by the Mössbauer spectroscopy. The possibility of different states for the Fe atoms can be assumed from the hyperfine parameters, which are the isomer shift (IS) and hyperfine magnetic field (B_{hf}).

Figure 3 presents transmission Mössbauer spectra of studied metallic glasses. The spectra are composed of six well defined, but broadened lines, which are characteristic features of amorphous ferromagnetic alloys.

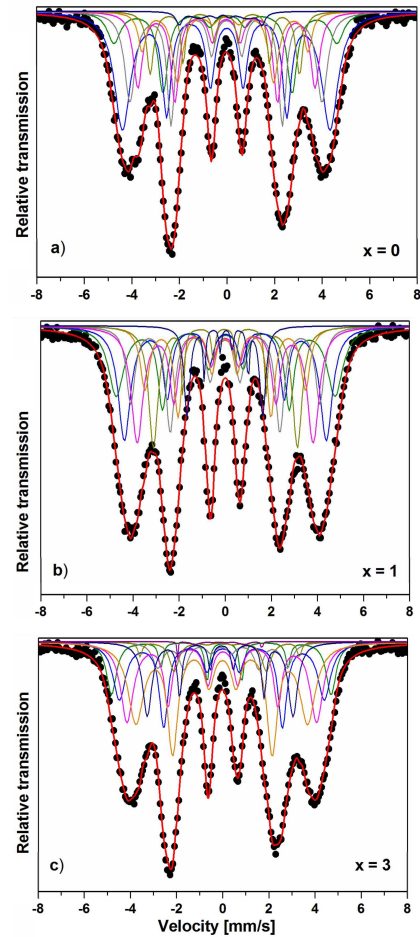


Fig. 3. Transmission Mössbauer spectra and their fits for $(\text{Fe}_{0.75}\text{B}_{0.15}\text{Si}_{0.1})_{100-x}\text{Zr}_x$ glasses: $x = 0$ (a), $x = 1$ (b), $x = 3$ (c).

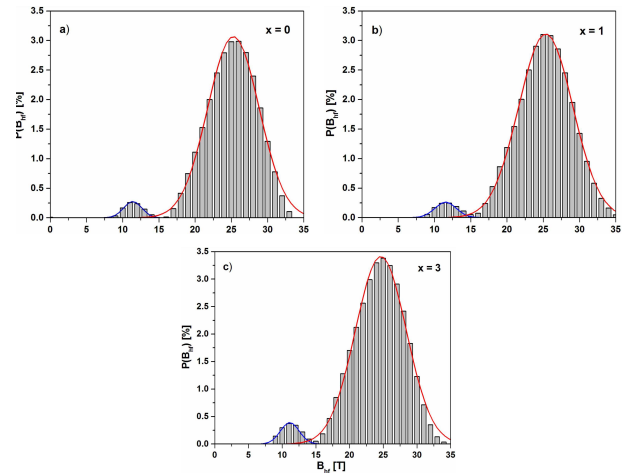


Fig. 4. Hyperfine field distribution of $(\text{Fe}_{0.75}\text{B}_{0.15}\text{Si}_{0.1})_{100-x}\text{Zr}_x$ metallic glasses: $x = 0$ (a), $x = 1$ (b), $x = 3$ (c).

The corresponding hyperfine magnetic field distributions are presented in Fig. 4. The broad distributions are connected with different local surroundings of the Fe atoms. Moreover, bimodal hyperfine field distributions

with the low- and high-field components can be observed. Basing on the results presented by Brzózka et al. [8] the bimodal behavior of B_{hf} distributions could be interpreted in terms of existence of at least two different Fe local environments. The high-field component is associated with regions of iron atoms, which are partially surrounded by the atoms of paramagnetic elements (Zr and B) in the first coordination sphere. The low-field component is characterized by areas rich in iron. Similar decomposition was obtained for $Fe_{61}Co_{10}Zr_5W_4B_{20}$ bulk metallic glass by Pawlik [9].

TABLE II

Hyperfine parameters of $(Fe_{0.75}B_{0.15}Si_{0.1})_{100-x}Zr_x$ alloys. B_{hf} — hyperfine magnetic field, IS — isomer shift, A — relative area.

x [at.%]	B_{hf} [T]	IS [mm/s]	A [%]
0	29.1	-0.011	15
	27.1	-0.010	30
	25.1	-0.018	19
	23.2	-0.016	15
	21.6	-0.06	12
	19.4	-0.048	5
	10.8	-0.026	4
1	29.4	0.142	20
	27.1	0.133	19
	25.4	0.114	19
	23.7	0.112	21
	21.6	0.103	13
	19.4	0.108	5
	10.2	0.132	3
3	29.5	-0.004	5
	27.5	-0.023	20
	25.4	-0.025	20
	23.1	-0.037	35
	21.4	-0.129	4
	19.6	-0.088	6
	17.4	-0.048	7
	11.3	0.144	3

The Mössbauer measured spectra were decomposed into 7 (for $x = 0, 1$) and 8 (for $x = 3$) subspectra. The data of IS and B_{hf} are listed in Table II. Table II presents also the area under the subspectra (A). The subspectra are related to random distribution of B and Zr atoms in the nearest neighborhood. Such ordering of atoms allows to form Fe-based clusters with specific configurations of magnetic moments. Torrens-Serra et al. [10] reported that the high-field distributions of B_{hf} field (10, 18, 24, and 33 T) for Fe–B–Nb metallic glasses should be attributed to the presence of a Fe–B environment. Therefore, the calculated values of hyperfine magnetic fields of each subspectra can be related to existing environment rich in paramagnetic atoms. The addition of Zr atoms (for $x = 3$ alloy) caused the increase of subspectra number with high value of hyperfine magnetic field. It also caused a reducing of Fe–Fe pairs and a formation of Fe–B and Fe–Zr atomic pairs.

The decrease of the coercivity is also believed to result from a higher interaction between Fe atoms due to the slightly increased interatomic distance Fe–Fe formed by the addition of Zr, which has larger atomic size than Fe.

4. Conclusions

The as-cast Fe-based alloys seem to be good magnetic materials, therefore the effect of Zr addition on structure and selected magnetic properties of $Fe_{75}B_{15}Si_{10}$ metallic glasses was examined. The lowest coercivity was obtained for the alloy with 3 at.% Zr addition. The Mössbauer spectra of glassy ribbons show broadened sextet patterns typical for the structural disorder of amorphous ferromagnetic materials. Different local environments of the Fe atoms were proposed, characterized by at least eight different hyperfine parameters. The addition of Zr atoms in $Fe_{75}B_{15}Si_{10}$ alloy probably allows to extend the Fe–Fe distances and reduce a number of Fe–Fe pairs, which is connected with H_c value. Reduction of H_c value from 247 A/m to 64 A/m is associated with the formation of Fe–Zr, B–Zr and Si–Zr pairs in amorphous alloy. The substitution of Fe by Zr in a disordered magnetic Fe-based structure led to the increase of paramagnetic environments [11,12]. This change is associated with a reduction in the amount of delocalized $3d$ electrons responsible for the ferromagnetism.

Acknowledgments

This publication was financed by the Ministry of Science and Higher Education of Poland as the statutory financial grant of the Faculty of Mechanical Engineering SUT in 2016.

References

- [1] W. Pilarczyk, *Cryst. Res. Technol.* **50**, 700 (2015).
- [2] P. Gebara, P. Pawlik, B. Michalski, J.J. Wysocki, K. Kotynia, *Acta Phys. Pol. A* **128**, 87 (2015).
- [3] R. Babilas, M. Kądziołka-Gaweł, A. Burian, L. Temleitner, *J. Magn. Magn. Mater.* **406**, 171 (2016).
- [4] A. Inoue, B. Shen, *Mater. Trans.* **43**, 2350 (2002).
- [5] Y. Geng, Y.W.J. Qiang, G. Zhang, C. Dong, O. Tegus, J. Sun, *Intermetallics* **67**, 138 (2015).
- [6] E. Axinte, *Mater. Des.* **35**, 518 (2012).
- [7] R.A. Brand, *WinNormos-for-Igor Users Manual Version 3.0*, Universität Duisburg, Duisburg 2009.
- [8] K. Brzózka, A. Ślawska-Waniewska, K. Jezuita, *J. Magn. Magn. Mater.* **160**, 255 (1996).
- [9] P. Pawlik, *J. Alloys Comp.* **423**, 96 (2006).
- [10] J. Torrens-Serra, P. Bruna, J. Rodríguez-Viejo, T. Pradell, M.T. Clavaguera-Mora, *Rev. Adv. Mater. Sci.* **18**, 464 (2008).
- [11] A. Grabias, M. Kopcewicz, D. Oleszak, *J. Alloys Comp.* **339**, 221 (2002).
- [12] M. Kopcewicz, A. Grabias, J. Latuch, M. Kowalczyk, *Mater. Chem. Phys.* **126**, 669 (2011).